Structure and charge-ordering transition in Bi-based bilayered $Bi_{0.44}Ca_{2.56}Mn_2O_7$ manganite

Y. L. Qin,[1] J. L. García-Muñoz,[2] H. W. Zandbergen,[1] and J. A. Alonso[3]
[1]*National Center for HREM, Laboratory of Materials Science, Delft University of Technology, Rotterdamseweg 137, 2628 AL Delft, The Netherlands*
[2]*Institut de Ciència de Materials de Barcelona, CSIC, Campus de la UAB, E-08193 Bellaterra, Spain*
[3]*Instituto de Ciencia de Materiales de Madrid, CSIC, Cantoblanco, E-28049 Madrid, Spain*
(Received 11 August 2000; published 21 March 2001)

The normal and charge-ordered phases in $Bi_{2-2x}Ca_{1+2x}Mn_2O_7$ with a hole-doping level of $x=0.78$ have been investigated by transmission electron microscopy. $Bi_{0.44}Ca_{2.56}Mn_2O_7$, the first identified member of the 327-type Bi-Ca-Mn-O family, was obtained under high oxygen pressure, and presents an orthorhombic structure with *Amam* symmetry at room temperature. A structural modulation is observed in this unusual layered manganite below 210 K, characterized by the one-dimensional wave vector $\mathbf{q}=0.22\mathbf{b}^*$ and a single transverse component. At low temperature the superspace group of the charge ordered state is P_{s-11}^{Amam}.

DOI: 10.1103/PhysRevB.63.144108 PACS number(s): 71.45.Lr, 68.37.Lp, 71.38.−k, 71.27.+a

I. INTRODUCTION

Manganese oxides $Ln_{1-x}A_xMnO_3$ (Ln=trivalent lanthanide, A=divalent Ca, Sr, Ba) have attracted tremendous attention because they exhibit wide variety of fascinating physical properties, such as colossal magnetoresistance (CMR) effect,[1–4] magnetostructural effects,[5] magnetic polarons,[6] and charge ordering (CO).[7]During the last years extensive studies are reported on the factors controlling the migration of conductive e_g electrons (or e_g holes) in perovskite manganese oxides. In particular, charge/orbital ordering (CO/OO) of manganese can be rationalized by considering the behavior of e_g electrons in the manganese $3d$ orbitals, strongly bonded to $2p$ oxygen ones. The tendency showed by many manganites, as well as by other transition-metal oxides, of a real space ordering of the charge carriers is especially remarkable at some fractional values of the doping level x, mainly $x=\frac{1}{2}$. More complex orbital and charge orderings are observed for hole doping $x>\frac{1}{2}$, which are being the subject of a growing research effort. For $x>0.50$ commensurate with large repeat period and incommensurate modulations are being reported.[8,9] So far, most of the research work has been devoted to ABO_3-type compounds, the $n=\infty$ member of the Ruddlesden and Popper $(Ln\text{-}A)_{n+1}Mn_nO_{3n+1}$-like series.[7–11]

Recently, investigations have focused on the layered perovskites $(La\text{-}A)_{n+1}Mn_nO_{3n+1}$ (A=Sr, Ca) with $n\neq\infty$. Studies on $La_{2-2x}A_{1+2x}Mn_2O_7$ ($n=2$) manganites have shown a very high CMR effect for the doping concentrations $0.2\leqslant x\leqslant 0.5$.[12–14] The natural stacking of perovskite bilayers in these phases represents an excellent opportunity for tunnelling or spin valves based devices and therefore have attracted substantial interest.[12–18] Superstructures interpreted in terms of the d_Z^2 orbital ordering of Mn^{3+} associated to a charge-ordered phase have been observed in $(La,Sr)_2MnO_4$ ($n=1$) (Refs. 18 and 19) and $LaSr_2Mn_2O_7$ ($n=2$) materials.[20,21] The latter with a hole-doping level of $x=0.5$. To date, the scarce CO and OO studies on $n=2$ layered manganites refer to materials having half doped bilayers ($x=0.50$). Typically these studies involve the use of electron diffraction, neutron scattering, or/and x-ray scattering techniques.[8,9,22] The orbital ordering observed in $LaSr_2Mn_2O_7$ ($T_{CO}=210$ K) is essentially identical to that of $La_{1/2}Ca_{1/2}MnO_3$. However, the charge/orbital ordered state of $LaSr_2Mn_2O_7$ collapses again with decreasing temperature below 100 K, and the *A*-type antiferromagnetic-state is the stable phase at low temperature.[21]

Studies of charge-stripe formation in $n=2$ layered perovskites in the Mn^{4+} rich regime (with a doping concentration $x>0.5$) are lacking. Furthermore, most of the $(Ln\text{-}A)_3Mn_2O_7$ samples previously grown and investigated were based on Ln=La, Pr, or Nd. Logically, an overall comprehension of this family of materials requires extending the investigations to the other members, particularly, those with small lanthanides. The ionic radius ($\langle r_0\rangle^{IX}=1.16$ Å) that Bi^{3+} ions adopt in $Bi_{1/2}Ca_{1/2}MnO_3$, for instance, is considerably shorter than the size of the lanthanide in the previously reported $Ln_{2-2x}Ca_{1+2x}Mn_2O_7$ phases. Decreasing the size of the large cation, however, the difficulties found in the synthesis are more severe.

In this paper we report the direct observation of a charge-ordered layered $Bi_{2-2x}Ca_{1+2x}Mn_2O_7$ phase with $x\approx 0.78$, close to $Mn^{3+}/Mn^{4+}=\frac{1}{4}$. During a study of the manganite perovskite $Bi_{1/4}Ca_{3/4}MnO_3$,[23] a different layered Bi based phase with $a\cong b=0.53$ nm and $c=1.918$ nm was identified by means of electron diffraction and high-resolution electron microscopy (HREM) experiments. It is of interest to recall that the presence of Bi as trivalent lanthanide is known to produce unconventional charge, spin, and lattice dynamics in some charge-ordered phases of $(Bi,Ca)MnO_3$ oxides.[24–26] Moreover, it is worth noticing that the high doping level of the present $n=2$ bilayer phase is still not well described and understood in the infinite layer $(Ln,Ca)MnO_3$ systems. Using transmission electron microscopy techniques, we have characterized the structural features of normal and charge-ordered phases in the highly doped layered $Bi_{0.44}Ca_{2.56}Mn_2O_7$ oxide.

II. EXPERIMENT

A black polycrystalline sample was synthesized under oxygen pressure from high-purity powders of Bi_2O_3, $CaCO_3$,

and Mn_2O_3, mixed in the proportion corresponding to Bi(0.25)-Ca(0.75)-Mn-O(3). Prior to use the powders were dehydrated at 900 °C for 12 h. The stoichiometric mixture was thoroughly grounded in an agate mortar and pressed into a pellet. After several intermediate sintering temperatures (in an alumina crucible) with intermediate grindings, the sample was pressed into a pellet and finally annealed at 1100 °C under 200-bar oxygen pressure for 24 h. The sample was then cooled to room temperature at a rate of 300 °C per hour. Thin specimens for electron microscopy were prepared simply by crushing the sample with an agate mortar and pestle. Crushed fragments were mixed with ethanol and then deposited onto a Cu grid coated with a thin carbon film. Electron microscopy was performed with a Philips CM30T transmission electron microscope equipped with a low-temperature sample stage, operating at 300 kV. A Philips CM30UT-FEG electron microscope with a Link EDX detector was also used for quantitative analysis.

Two different phases were observed. The main nominal phase $Bi_{0.25}Ca_{0.75}MnO_3$ of polycrystalline sample was found to be orthorhombic at room temperature, with Pnma symmetry and a $\sqrt{2}a_p$, $2a_p$, $\sqrt{2}a_p$ enlarged unit cell, where a_p is the simple perovskite lattice parameter. At low temperature, down to 110 K, we did not observe charge-ordered domains associated to this phase. In contrast, a temperature dependent behavior was observed in the grains containing the 327 phase. The composition determination of the new orthorhombic Bi-Ca-Mn-O phase was performed by a quantitative EDX using a spot size of about 20 nm in the Philips CM30UT electron microscope. Quantitative analysis averaging over several locations and grains results in a Bi/Ca/Mn atomic percentage ratio of 5.0/29.1/22.6. These ratios indicate that the phase has a composition corresponding to $Bi_yCa_{3-y}Mn_2O_7$ with $y=0.44$. For the sake of clarity it is more convenient writing the stoichiometry as $Bi_{2-2x}Ca_{1+2x}Mn_2O_7$ since, in this description, x directly represents the concentration of Mn^{4+} ions (holes) in the bilayers. The average x value determined for the 327 phase was $x=0.78$, a doping level close to nominal commensurate value $\frac{3}{4}$. The present work focuses on the structural properties and charge ordering phenomena in this highly doped bilayered manganite.

III. RESULTS AND DISCUSSION

$Bi_{0.44}Ca_{2.56}Mn_2O_7$ crystals were first characterized at room temperature (RT) by conventional selected area diffraction using a parallel electron beam in order to determine the crystal symmetry. The main zonal electron diffraction patterns (EDP's) prove the phase to have orthorhombic symmetry. Figures 1(a)–(f) show the selected area EDP's of $Bi_{0.44}Ca_{2.56}Mn_2O_7$ phase along [100], [110], [001], [010], [101], and [011] zone axes, respectively. Indexation of these EDP's shows that it exhibits an *A*-centered orthorhombic structure. The observed reflections in all the diffraction patterns are limited by the reflection conditions: $k+l=2n$ for hkl and $0kl$, h, $l=2n$ for hol and $k=2n$ for $hk0$. The extinction condition along **a*** is $h=2n+1$. The weak spots of $(h00)$ with $h=2n+1$ in Figs. 1(c) and (f) are due to the multiple scattering. When we tilted the sample away from the low-index zone to minimize multiple scattering, the $(h00)$ $(h=2n+1)$ reflections disappeared. Therefore the possible space groups for the $Bi_{0.44}Ca_{2.56}Mn_2O_7$ phase are limited to $Ama2$ (40), $A2_1am$ (36), or *Amam* (63). In addition, further convergent-beam electron diffraction (CBED) experiments show that there are mirror planes perpendicular to the *a*, *b*, and *c* axes. Hence these diffraction data suggest the space group to be *Amam*.

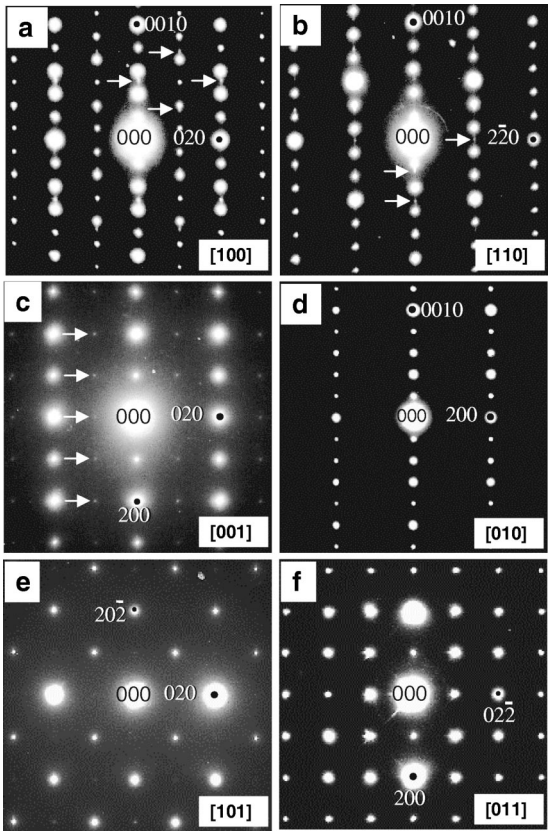

FIG. 1. Electron-diffraction patterns of $Bi_{0.44}Ca_{2.56}Mn_2O_7$ phase obtained along (a) [100], (b) [110], (c) [001], (d) [010], (e) [101], and (f) [011] zone axes. The extra weak reflections can be indexed as the normal $\sqrt{2}a_p$, $2a_p$, $\sqrt{2}a_p$ orthorhombic cell with *Pnma* symmetry.

Besides the main spots that belong to *A*-centered orthorhombic structure, some extra weak reflections can also be seen in the EDP's taken at RT [marked by arrowheads in Figs. 1(a)–(c)]. They can be indexed as the normal $\sqrt{}a_p$, $2a_p$, $\sqrt{}a_p$ primitive orthorhombic structure of ABO_3 type. The orientational relationship between matrix *A*-centered (*A*) $Bi_{0.44}Ca_{2.56}Mn_2O_7$ and the primitive (*P*) orthorhombic structure is the following: $[100]_A//[100]_P$, $(010)_A//(001)_P$, and $(001)_A//(010)_P$. The present $Bi_{0.44}Ca_{2.56}Mn_2O_7$ crystal contains small amounts of the ABO_3 type ($\sqrt{2}a_p\times 2a_p \times\sqrt{2}a_p$) structure in the form of lamellae intergrowths in the *A*-centered orthorhombic structure. An example of this intergrowth is displayed in Fig. 2(a), showing a $[110]_A$ zone-axis HREM image. Figure 2(b) shows an enlarged HREM image of the area outlined in Fig. 2(a). In this image the (Bi, Ca) and Mn atoms positions can be recognized as dark dots, and

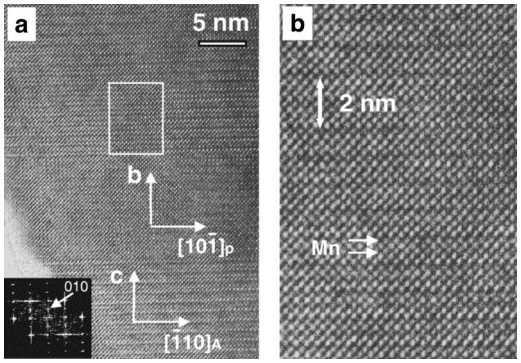

FIG. 2. (a) High-resolution image at room temperature taken along the $[110]_A$ direction. It illustrates the intergrowth of the *A*-centered orthorhombic $Bi_{0.44}Ca_{2.56}Mn_2O_7$ structure with lamellae of the *Pnma* $Bi_{1-x}Ca_xMnO_3$ phase. The Fourier transform of the *Pnma* orthorhombic lamellae along the $[110]_A$ or $[101]_P$ direction is superimposed onto the HREM image. It confirms the $\sqrt{2}a_p$, $2a_p$, $\sqrt{2}a_p$ orthorhombic structure. (b) Enlarged view of the area outlined in (a), showing the 327-type layered structure of the $Bi_{0.44}Ca_{2.56}Mn_2O_7$ phase along the *c* direction.

the bilayered structure of the $(Ln\text{-}M)_3Mn_2O_7$ phase along the *c* axis can be clearly observed. Hence HREM and electron-diffraction data give evidence of large regions of well-crystallized and defined 327-type layered structure of the $Bi_{0.44}Ca_{2.56}Mn_2O_7$ phase.

The *a* and *b* axes can be taken the *a* and *c* axes of the Pnma $\sqrt{2}a_p$, $2a_p$, $\sqrt{2}a_p$ primitive orthorhombic structure because the HREM image of an intergrowth in Fig. 2(a) shows a fully coherent interface. We assume that the intergrowth primitive orthorhombic phase has the same unit cell as the main nominal phase $Bi_{0.25}Ca_{0.75}MnO_3$ in the polycrystalline sample, which has been determined in Ref. 23. The lattice parameter along the *c* axis was determined from ratio of the spacings of $00l$ and $0h0$ reflections. This all gives the cell parameters to be $a=0.534\,846$ nm, $b=0.531\,941$ nm, and $c=1.918$ nm.

Electron diffraction was also performed at low temperatures, in the range 100–300 K, to investigate the presence of charge ordering in the $Bi_{0.44}Ca_{2.56}Mn_2O_7$ phase. Figure 3(a) shows the [001] zone-axis EDP of $Bi_{0.44}Ca_{2.56}Mn_2O_7$ taken

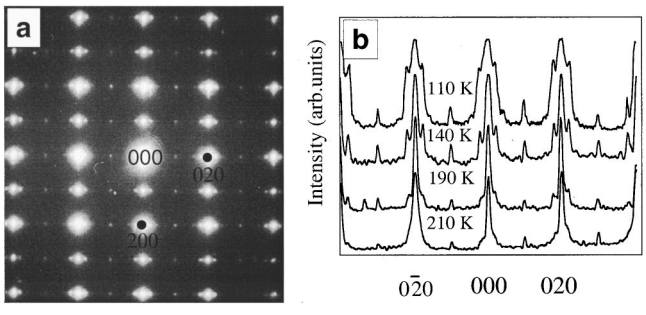

FIG. 3. (a) [001] zone-axis electron-diffraction pattern of $Bi_{0.44}Ca_{2.56}Mn_2O_7$ phase obtained at 110 K. The superlattice spots can be clearly seen. (b) Microphotometric density curves along the b^* direction showing the temperature variation of the superstructure reflections.

at 110 K. Due to our limited accuracy in unit-cell determination, an appreciable change in lattice parameters was not observed from the original orthorhombic lattice by cooling. Evidence for a long period structure related to a charge-ordered state is given by the appearance of sharp superlattice spots around each fundamental Bragg reflection in the [010] direction. It is found that the structural modulation is incommensurate, the superlattice spots being at the positions $(h, 2k\pm0.22, 0)$. The corresponding wave vector can be written as $\mathbf{q}=\mathbf{b}^*[0,\delta,0]$, where $\delta=0.22$. If we use the simple perovskite cell (cubic) as reference, **q** is along the [110] direction of the cubic perovskite structure. It can be thus written as $q=\delta/d$ with $d=\sqrt{2}a_p$. In order to investigate the temperature dependence of the superstructure reflections, different patterns were collected at several temperatures warming the sample from 110 K up to RT (300 K). Line plots across reflections including superreflections were made using digitalized images of diffraction patterns recorded on the photograph films. The curves along the $\mathbf{b}^*$ direction taken at 110, 140, 190, and 210 K are shown in Fig. 3(b). Note that the temperature of the investigated crystal is actually not measured but rather a position about 10 mm from the specimen cup such that the real temperature of the crystal is higher than the indicated temperature. A decrease of the intensities of the superlattice spots is clearly observed with increasing temperature. They become invisible around 210 K. No distinguishable changes in the crystal symmetry or the length of **q** were observed with increasing temperature.

It is interesting to recall that Li *et al.*[27] observed two distinctive structural modulations in the charge-ordered phase of tetragonal $LaSr_2Mn_2O_7$ (along $\mathbf{a}^*$ and $\mathbf{b}^*$ directions, respectively). They were considered to originate from twin domains with wave vectors rotated by 90°.[19,20,26] In the present orthorhombic phase only one set of superstructure reflections was detected [Fig. 3(a)].

Following the method of describing incommensurate superstructures by de Wolff *et al.*,[28] the one-dimensionally modulated structure of this charge-ordered phase can be described using a four-dimensional superspace group. Apart from the three reciprocal basis vectors a fourth vector describing the modulation ($\mathbf{q}=\delta\mathbf{b}^*$) is added. With this the reciprocal-lattice vectors for the CO phase can be expressed as $\mathbf{H}=H\mathbf{a}^*+K\mathbf{b}^*+L\mathbf{c}^*+m\mathbf{q}$, where *H*, *K*, *L*, and *m* are integers. The systematic extinction conditions associated with this one-dimensionally modulated structure are observed to be the following: $K+L=2n$ in general, $H=2n$ for *H0L0*, and $m=2n$ for $0KLm$. Thus from the general extinction condition we can conclude that the four-dimensional superspace group belongs to the Bravais class P^{Ammm}_{11-1} (No. 15).[28] The possible superspace group of the CO phase of $Bi_{0.44}Ca_{2.56}Mn_2O_7$ can be determined as P^{Ama2}_{s-1-1} or P^{Amam}_{s-11} [$Ama2(0p0)s00$ or $Amam(0p0)s00$ in one-line symbol] with the use of Superspace Group Tables.[29] This would result in the $Ama2$ or $Amam$ as space group for the average structure. Since no symmetry difference between the basic structure of the low-temperature phase and that of the RT phase was found in the CBED experiments, the superspace group of $Bi_{0.44}Ca_{2.56}Mn_2O_7$ phase is suggested to be

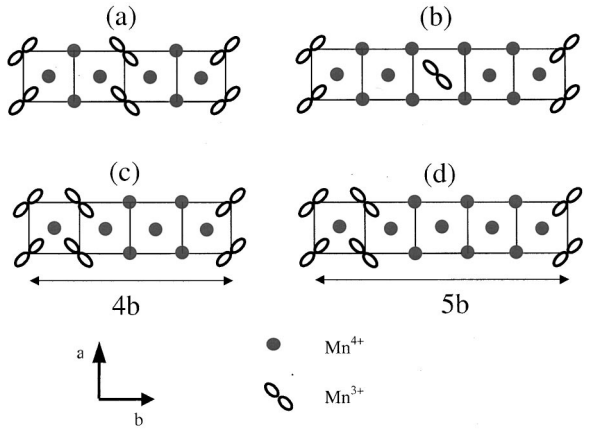

FIG. 4. Schematic representations of possible Mn^{3+}-Mn^{4+} charge-ordering and $d_{3x^2-r^2}/d_{3y^2-r^2}$ orbital-ordering of Mn^{3+} projected along the [001] direction for $x=\frac{3}{4}$ [(a) and (c)] and $x=\frac{4}{5}$ [(b) and (d)] corresponding, respectively, to the Wigner-crystal and bistripe models.

P_{s-11}^{Amam}. For *HKLm*, the reflections with $m=2n$ are very weak and often not observable. Reflections with $m>2$ are not present at all. Thus only the $m=1$ superreflections are very significant. This indicates that the deviation from the average structure is close to sinusoidal. It is of interest to note that the intensities of the superstructure reflections in the higher-order Laue zones are observed to be relatively stronger than those of the super-reflections in the zero-order Laue zone. This will be the subject of further research.

In the investigated phase, $q=\delta/d=1/4d(1-\varepsilon)$ and the incommensurability parameter ε ($\varepsilon=0.092$) shows no temperature dependence. This is in agreement with a charge ordering as the origin of the incommensurability. Regarding the linear $\delta=0.22\approx 1-x$ dependence, the incommensurate super-reflection spots should be attributed to the mixed commensurate modulations $4b_0$ and $5b_0$. The adjacent commensurate configurations to the doping level $x=0.78$ are $x=\frac{3}{4}$ and $x=\frac{4}{5}$. A fine mixture of 40% $4b_0$ and 60% $5b_0$ paired periods is completely consistent with the overall periodicity $\mathbf{q}=0.22\mathbf{b}^*$. In Fig. 4 we show a schematic representation of the Wigner [Figs. 4(a) and (b)] and bistripe [Figs. 4(c) and (d)] models for the orbital- and charge-ordered superstructures with doping levels $x=\frac{3}{4}$ (0.75) and $x=\frac{4}{5}$ (0.80). In the bistripe models the pattern has the form of stable pairs of heavily Jahn-Teller distorted diagonal $Mn^{3+}O_6$ stripes, separated periodically by stripes of nondistorted $Mn^{4+}O_6$ octahedra. If the priority is to minimize the Coulomb energy, the Wigner model should be considered.[30] In the model of paired Jahn-Teller stripes (JTS) longitudinal displacements are expected from the fact that bistripe and background regions may have different lattice spacings.[8] Based on image simulations, quantitative electron diffraction, and high-resolution imaging, a careful crystallographic study of $La_{0.33}Ca_{0.67}MnO_3$ has been reported in Ref. 31, supporting the Wigner-crystal model. The authors show that the large longitudinal displacement of the bistripe model is incompatible with electron-diffraction data. Further work is required to investigate the expected longitudinal displacements in the bistripe model of bilayered perovskites. In principle, the superstructure could be different in the various members of the Ruddlesden-Popper series because the presence of rock-salt-type layers between the perovskite blocks can lead to another compromise between minimizing the Coulomb repulsion of the charges (Wigner crystal) and the lattice strain associated with orbital ordering (bistripe models).

In summary, we have reported the observation of a 327-type layered structure in the Bi-Ca-Mn-O phase diagram ($n=2$ member of the Ruddlesden-Popper $(Bi,Ca)_{n+1}Mn_nO_{3n+1}$ series), obtained under high oxygen pressure. The normal and charge-ordered structures of $Bi_{0.44}Ca_{2.56}Mn_2O_7$ have been investigated by transmission-electron-microscopy and HREM measurements. At room temperature its crystal structure presents *Amam* symmetry. Of special interest is the high doping level of the present Bi-based bilayered manganite, $x=0.78$. Electron-diffraction data reveal the appearance of a superstructure below 210 K. The structural modulation in the low-temperature phase of this layered manganite corresponds the one-dimensional wave vector $\mathbf{q}=0.22\mathbf{b}^*$ and presents a single transverse component. The modulated structure has been successfully explained in terms of mixed domains of $4b_0$ and $5b_0$ periodicity associated with the $d_z2(Mn^{3+})$ orbital ordering. The superspace group of CO state is determined to be P_{s-11}^{Amam}.

ACKNOWLEDGMENTS

The authors acknowledge financial support by Stichting voor Fundamenteel Onderzoek der Materie (FOM), MEC (PB97-1175), Generalitat de Catalunya (GRQ95-8029), INTAS (Project No. 971-11954), and the EC through the ''Oxide Spin Electronics (OXSEN)'' network (TMR).

[1] K. Chahara, T. Ohno, M. Kasai, and Y. Kozono, Appl. Phys. Lett. **63**, 1990 (1993).
[2] R. von Helmolt, J. Weckerg, B. Holzapfel, L. Schultz, and K. Samwer, Phys. Rev. Lett. **71**, 2331 (1993).
[3] S. Jin, T. H. Tiefel, M. McCormack, R. A. Fastnacht, R. Ramesh, and L. H. Chen, Science **264**, 413 (1994).
[4] C. N. R. Rao and A. K. Cheetham, Science **272**, 369 (1996).
[5] A. Asamitsu, Y. Moritomo, Y. Tomioka, T. Arima, and Y. Tokura, Nature (London) **373**, 407 (1995).
[6] J. M. De Teresa, M. R. Ibarra, P. A. Algarabel, C. Ritter, C. Marquina, J. Blasco, J. Garcia, A. del Morl, and Z. Arnold, Nature (London) **386**, 256 (1997).
[7] Y. Tomioka, A. Asamitsu, Y. Moritomo, H. Kuwahara, and Y. Tokura, Phys. Rev. Lett. **74**, 5108 (1995).
[8] S. Mori, C. H. Chen, and S.-W. Cheong, Nature (London) **392**, 473 (1998).
[9] P. G. Radaelli, D. E. Cox, L. Capogna, S.-W. Cheong, and M. Marezio, Phys. Rev. B **59**, 14 440 (1999).

[10] H. Kuwahara, Y. Tomioka, A. Asamitsu, Y. Moritomo, and Y. Tokura, Science **270**, 961 (1995).
[11] C. N. R. Rao, A. Arulraj, P. N. Santosh, and A. K. Cheetham, Chem. Mater. **10**, 2714 (1998).
[12] Y. Moritomto, A. Asamitsu, H. Kuwahara, and Y. Tokura, Nature (London) **380**, 141 (1996).
[13] T. Kimura, Y. Tomioka, H. Kuwahara, A. Asamitsu, M. Tamura, and Y. Tokura, Science **274**, 1698 (1996).
[14] H. Asano, J. Hayakawa, and M. Matsui, Phys. Rev. B **68**, 5395 (1997).
[15] D. N. Argyriou, H. N. Bordallo, J. F. Mitchell, J. D. Jorgensen, and G. F. Strouse, Phys. Rev. B **60**, 6200 (1999).
[16] P. K. de Boer and R. A. de Groot, Phys. Rev. B **60**, 10 758 (1999).
[17] L. Vasiliu-Doloc, S. Rosenkranz, R. Osborn, S. K. Sinha, J. W. Lynn, J. Mesot, O. H. Seeck, G. Preosti, A. J. Fedro, and J. F. Mitchell, Phys. Rev. Lett. **83**, 4393 (1999).
[18] R. H. Heffner, D. E. MacLaughlin, G. J. Nieuwenhuys, T. Kimura, G. M. Luke, Y. Tokura, and Y. J. Uemura, Phys. Rev. Lett. **81**, 1706 (1998).
[19] Y. Moritomo, Y. Tomioka, A. Asamitsu, Y. Tokura, and Y. Matsui, Phys. Rev. B **51**, 3297 (1995).
[20] W. Bao, C. H. Chen, S. A. Carter, and S.-W. Cheong, Solid State Commun. **98**, 55 (1996).
[21] T. Kimura, R. Kumai, Y. Tokura, J. Q. Li, and Y. Matsui, Phys. Rev. B **58**, 11 081 (1998).
[22] Y. Su, C-H. Du, P. D. Hatton, S. P. Collins, and S-W. Cheong, Phys. Rev. B **59**, 11 687 (1999).
[23] J. L. García-Muñoz, A. Llobet *et al.* (unpublished). See also A. Llobet, C. Frontera, J. L. García-Muñoz, C. Ritter, and M. A. G. Aranda, Chem. Mater. **12**, 3648 (2000); J. L. García-Muñoz, C. Frontera, M. A. G. .Aranda, A. Llobet, and C. Ritter, Phys. Rev. B **63**, 064415 (2001).
[24] W. Bao, J. D. Axe, C. H. Chen, and S. W. Cheong, Phys. Rev. Lett. **78**, 543 (1997).
[25] S. Yoon, M. Rübhausen, S. L. Cooper, K. H. Kim, and S-W. Cheong, cond-mat/0003250 (unpublished).
[26] H. Chiva, M. Kikuchi, K. Kusaba, Y. Muraoka, and Y. Syono, Solid State Commun. **99**, 499 (1996).
[27] J. Q. Li, Y. Matsui, T. Kimura, and Y. Tokura, Phys. Rev. B **57**, R3205 (1998).
[28] P. M. De Wolff, T. Janssen, and A. Janner, Acta Crystallogr., Sect. A: Cryst. Phys., Diffr., Theor. Gen. Crystallogr. **37**, 625 (1981).
[29] Via Internet from Yamamoto (http://www.nirim.go.jp/~yamamoto)
[30] E. P. Wigner, Phys. Rev. **46**, 1002 (1934).
[31] R. Wang, J. Gui, Y. Zhu, and A. R. Moodenbaugh, Phys. Rev. B **61**, 11 946 (2000).